



&lt;Research Article&gt;

## Fluorescent calcite distribution in the mammillary knobs of chicken eggshell's inner surface

Toshio Okazaki\*

**Summary** Low amounts of protoporphyrin IX (PPIX) are distributed both on the outside and inside of the chicken eggshell. However, when the inside of the eggshell was irradiated with near-ultraviolet light, it emitted fluorescence at 400–500 nm, corresponding to a different wavelength compared to the conventional PPIX emission at 635 and 678 nm. In this study, I aimed at elucidating the origin of this 400–500 nm fluorescent emission. The 400–500 nm broad peak was pronounced at the beginning of embryonic development and decreased as the mammillary knobs dissolved. Subsequent observations under a fluorescence microscope, following irradiation of the eggshell's inner surface with excitation light of 340–390 nm, confirmed the emission of blue fluorescence, and the fluorescence intensity decreased in line with the embryonic development. Furthermore, Raman spectroscopy and energy dispersive X-ray elemental analysis of the eggshell's inner surface revealed that the mammillary knobs were composed of calcite crystals and contained trace amounts of magnesium ions. These results indicated that the mammillary knobs were composed of fluorescent magnesium calcite crystals.

**Key words:** Eggshell, Mammillary knobs, Ultraviolet light, Fluorescence, Calcite

### 1. Introduction

Biom mineralization is the process through which living organisms produce minerals such as calcium phosphate  $\text{Ca}_3(\text{PO}_4)_2$  and calcium carbonate  $\text{CaCO}_3$ <sup>1</sup>. In humans, osteoblasts produce  $\text{Ca}_3(\text{PO}_4)_2$  through biom mineralization to form bones and teeth<sup>2</sup>, and birds create hard  $\text{CaCO}_3$  shells to protect the embryos inside their eggs<sup>3</sup>. In the avian uterus, calcium ions are transported to the mineralization front on the eggshell membrane as amorphous  $\text{CaCO}_3$ , encapsulated in extracellular vesicles originating from uterine epithelial

cells<sup>3</sup>. Mineralization progresses around the core of the keratin fiber membrane, eventually forming each layer of the eggshell, such as the mammillary layer, palisade layer, and cuticle layer<sup>4</sup>. Many bird eggshells contain pigments like melanin, porphyrin, and biliverdin<sup>5, 6</sup>, which are thought to serve as defense mechanisms and protective components against bacterial invasion<sup>7</sup>. Chicken eggshells also contain protoporphyrin IX (PPIX), which emits red fluorescence with peaks around 635 and 678 nm when irradiated with near-ultraviolet light (UVA) at 365 nm<sup>8</sup>. The content of PPIX varies depending on the breed of chicken, with a decrease observed toward the inside of the eggshell. However, it

Department of Animal Health Technology, Yamazaki University of Animal Health Technology, Minami-osawa 4-7-2, Hachioji, Tokyo 192-0364, Japan.

\*Corresponding author: Toshio Okazaki, Department of Animal Health Technology, Yamazaki University of Animal Health Technology, Minami-osawa 4-7-2, Hachioji, Tokyo 192-0364, Japan.  
Tel: +81-42-653-0901  
Fax: +81-42-653-0902  
E-mail: t\_okazaki@yamazaki.ac.jp

Received for Publication: November 27, 2023

Accepted for Publication: January 29, 2024

remains relatively consistent in the innermost part of every eggshell<sup>5, 8</sup>. The eggshell mammillary layer dissolves during embryonic development, and the solubilized calcium ions are used as a material for embryonic bone formation<sup>9</sup>. To elucidate the relationship between eggshell dissolution and PPIX redox, scanning electron microscopic (SEM) observation and fluorescent spectral analysis of the dissolved inner surface of the eggshell were performed. However, I observed a high and broad peak between 400 and 500 nm, which was clearly different from the fluorescence spectrum of PPIX detected in previous studies<sup>8</sup>. This broad peak disappeared in parallel with the dissolution of the mammillary layer on the inner surface of the eggshell during embryonic development. These results indicated that the mammillary layer consisting of  $\text{CaCO}_3$  could potentially emit fluorescence.  $\text{CaCO}_3$  has three crystalline phases (i.e., calcite, aragonite, and vaterite) with different morphological structures<sup>10</sup>. Both biotic and abiotic processes could lead to  $\text{CaCO}_3$  formation<sup>11</sup>, and calcite and aragonite including trace elements or organic matter fluoresce upon UV light illumination<sup>12</sup>. Biomineralized  $\text{CaCO}_3$  has been observed in both prokaryotes and eukaryotes, but no fluorescent  $\text{CaCO}_3$  crystals have been reported so far, except for those in thermophilic bacteria<sup>13</sup>. If the mammillary layer of a chicken eggshell contains fluorescent  $\text{CaCO}_3$  crystals, this would correspond to the first discovery in eukaryotes such as vertebrates. Therefore, I designed this study to elucidate the origin of the aforementioned broad fluorescence peak emitted by the inner surface of the chicken eggshell.

## 2. Materials and Methods

### Materials

To observe the structural changes of the inner surface of the eggshell of Boris brown hens (*Gallus gallus domesticus*) during embryonic development, fertilized eggs were incubated at a temperature of 37.5°C and a humidity of 60%. I cracked the eggs at each developmental stage and removed the membrane from the inner surface of the eggshells (Fig. 1). Next, the inner surface of the eggshell at

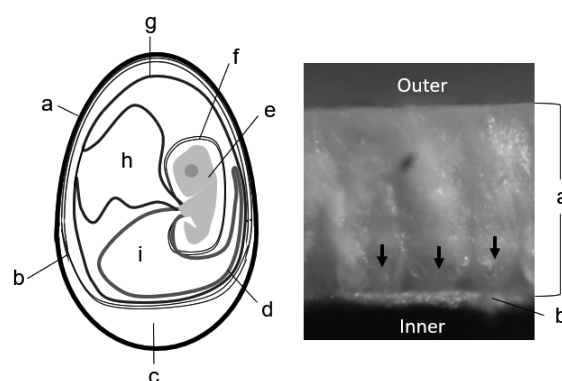


Fig. 1. Basic structure of the chicken egg and microscopic image of the eggshell (longitudinal section). a: eggshell; b: eggshell membrane; c: air cell; d: allantois; e: embryo; f: amnion; g: serosa; h: yolk sac; i: urine sac. The arrows in the photo indicate mammillary knobs inside the eggshell.

Table 1 Analytical procedure: devices and experimental purposes.

Device	Experimental purpose
SEM	Observation of eggshell dissolution (Fig. 2)
Mini-spectrometer	Analysis of fluorescence spectrum changes associated with eggshell dissolution (Fig. 3)
Fluorescent microscope	Observation of fluorescence properties of $\text{CaCO}_3$ crystal (Fig. 4)
Raman microscope	Calcite identification (Fig. 5A)
SEM-EDX	Elemental analysis of the calcite crystals (Fig. 5B)

each developmental stage was observed using an SEM and analyzed using a mini-spectroscope, fluorescence microscope, and Raman microscope for the purposes listed in Table 1.

SEM observation and energy dispersive X-ray elemental analysis of the mammillary knobs

The inner surface of the eggshell at each developmental stage was observed using a tabletop SEM (TM4000Plus, Hitachi, Tokyo, Japan). Concurrently, an elementary analysis of the eggshell's inner surface was performed using electron probe X-ray microanalysis (EDX).

Fluorescence spectrum analysis of eggshells during near-ultraviolet light (UVA) irradiation

The inner surface of the eggshell at each developmental stage was exposed to UVA at 365 nm using a UVGL-58 handheld UV lamp (Upland, CA, USA) in a dark room. Subsequently, fluorescence spectral analysis was conducted in the range of 400–750 nm using a Hamamatsu Photonics mini-spectrometer C11009MA (Hamamatsu, Shizuoka, Japan). The fluorescence spectrum intensity from the eggshell was measured as a relative reflectance ratio (A/D count ratio).

Fluorescence microscopic observation of the inner surface of eggshells

The inner surface of the eggshell at each developmental stage was observed using a fluorescence microscope BX53 (Olympus, Tokyo, Japan) after removing the eggshell membrane. For fluorescence microscopy, the excitation light intensity was kept the same and the following filter blocks were used: U-FUW: exciter, 340–390 nm; dichroic mirror, 410 nm; emitter, 420 nm; U-FBNA: exciter, 470–495 nm; dichroic mirror, 505 nm; emitter, 510 nm; U-FGW: exciter, 530–550 nm; dichroic mirror, 570 nm; and emitter, 575 nm.

Micro-Raman spectroscopy of the inner surface of the eggshell

Micro-Raman spectroscopy of the inside of the eggshell at each embryonic developmental stage on days 1 and 20 was performed using a Renishaw inVia™ Raman microscope (532 nm emission line of the Ar laser).

### 3. Results

Observation of the dissolution of eggshell mammillary knobs during chicken embryonic development using scanning electron microscopy

After removing the eggshell membrane, the inner surface of the eggshell was examined at each stage of embryonic development on the 1st, 11th, 16th, and 20th days (Fig. 1). The results showed that on the first day, the eggshell inner surface was intact. However, by the 11th day, the tips of the knobs had melted and become flat. By the 16th day, further melting had occurred, forming a hollow, and by the 20th day, the size of the hollow further expanded. These results confirmed that mammillary knobs on the inner surface of the eggshell dissolve during embryonic development.

Fluorescent spectrum analysis and fluorescent microscopic observation of the inner surface of chicken eggshells during embryonic development

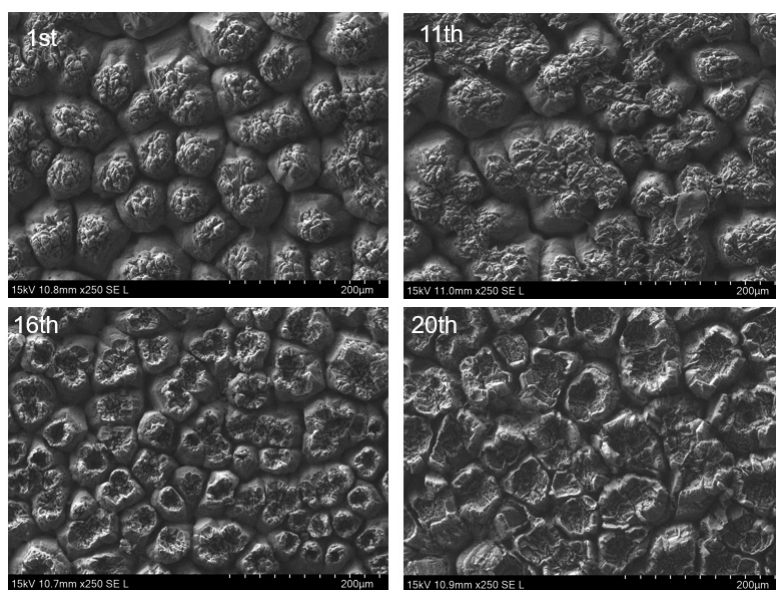


Fig. 2. Dissolution of the eggshell’s mammillary knobs during chicken embryonic development.

The days after the start of embryonic development are indicated in the upper left corner of the photographs.

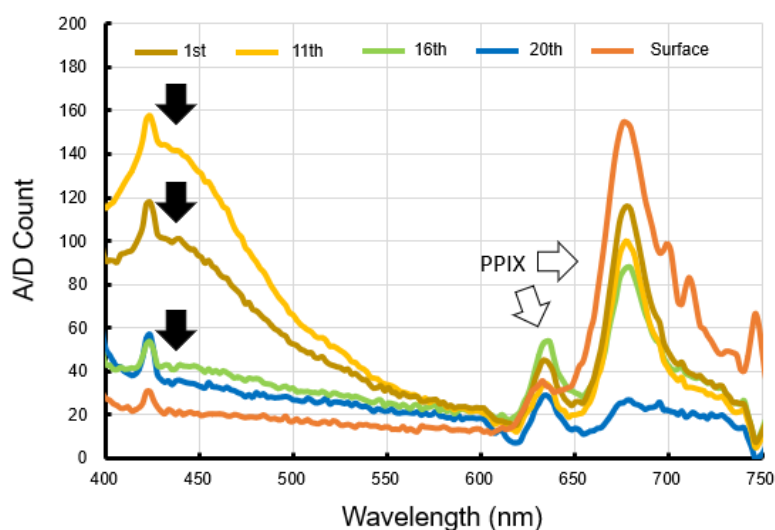


Fig. 3. Fluorescence spectral changes derived from the inner surface of the eggshell during embryonic development.

These data were obtained under 365-nm excitation light using a mini-spectrometer. The white arrows indicate PPIX peaks.

As shown in Fig. 2, the mammillary knobs dissolve during embryonic development. Therefore, I exposed the inner surface of chicken eggshells to UVA (365 nm) at each embryonic developmental stage and analyzed their emitted fluorescent spectra. On the 1st day, I observed a broad peak at 400–500 nm (black arrows in Fig. 3), along with peaks at 635 and 678 nm. The peaks at 635 and 678 nm are thought to be caused by protoporphyrin IX (PPIX)<sup>5,8</sup>. The peak at 400–500 nm was higher on the 11th day than on the 1st day and rapidly decreased on the 16th and 20th days. For comparison, when the fluorescence spectrum of the outer surface of the eggshell was analyzed, no peak was observed at 400–500 nm, and only peaks at 635 nm and 678 nm were observed (Fig. 3). Next, I observed the fluorescence derived from the inner surface of the eggshell at each embryonic developmental stage on days 1, 11, 16, and 20 using a fluorescence microscope. I confirmed blue fluorescence under 340–390-nm excitation (U-FUW filter condition), corresponding to 400–500 nm, with reducing intensity in accordance with embryonic development (Fig. 4A). These results were similar to those of fluorescence spectral analysis upon 365 nm UVA irradiation (Fig. 3). Furthermore, I detected green and red fluorescence when exposing the samples to excitation light of 470–495 nm (U-FBNA

filter) and 530–550 nm (U-FGW filter), respectively. These fluorescence intensities also decreased by day 20 (Fig. 4B).

Micro-Raman spectroscopy and electron probe X-ray microanalysis of the inner surface of the eggshell

My fluorescent spectral analysis and fluorescent microscopic observations revealed that mammillary knobs emit unique fluorescence when exposed to a specific excitation light (Fig. 3). These results suggested that the mammillary knobs are composed of fluorescent  $\text{CaCO}_3$  crystals; therefore, I performed Raman spectroscopy and energy dispersive X-ray (EDX) elemental analysis on the inner surface of the eggshell on the 1st and 20th days of chicken embryonic development. The Raman spectroscopic analysis confirmed Raman shifts on the inner surface of the eggshell at 1,086, 712, 281, and 156  $\text{cm}^{-1}$  (Fig. 5A) on both the 1st and 20th days. These shifts closely matched the Raman shift data of calcite at 1,085, 712, 280, and 153  $\text{cm}^{-1}$  reported by Donnelly et al. (2017)<sup>15</sup>. Furthermore, the EDX elemental analysis of the inner surface of the eggshell revealed the detection of  $\text{CaCO}_3$  constituent elements: Ca, C, and O. Small amounts of Mg and Na were also detected on the inner surface of the eggshell on the 1st day. However, these trace elements had almost

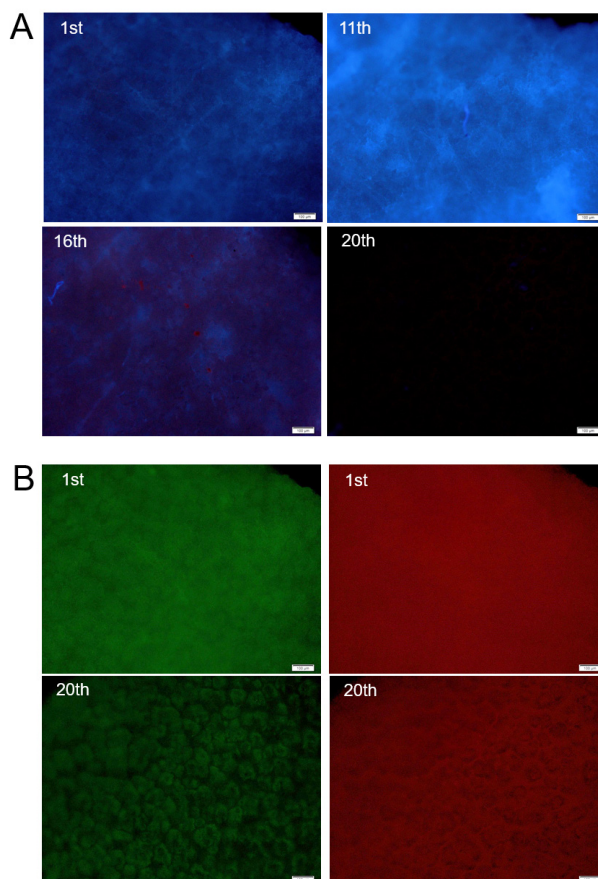


Fig. 4. Fluorescent intensity changes derived from the inner surface of the eggshell during embryonic development using a fluorescent microscope.  
 A: 340–390 nm excitation light; B: left, 470–495 nm excitation light; right, 530–550 nm excitation light.

disappeared or decreased by the 20th day (Fig. 5B). These data showed that the mammillary knobs are composed of the fluorescent magnesium calcite crystals.

#### 4. Discussion

The dissolution of the inner surface of eggshells during embryonic development, serving as material for bone formation, is a well-known phenomenon<sup>8,9</sup>. Scanning electron microscopy revealed the gradual scraping of mammillary knobs from the 1st to the 11th days, with further melting and the appearance of hollows on the 16th day. By the 20th day, the hollow had widened, resembling a large crater (Fig. 2). The near-UV light irradiation of the inner surface of the eggshell at different embryonic developmental stages revealed PPIX peaks at 635 and 678 nm, along with

400–500 nm broad peak, with the latter markedly decreasing during embryonic development (Fig. 3). My fluorescent microscopic observation of the inner surface of the eggshell upon irradiation with 340–390 nm excitation light revealed blue fluorescence with decreasing intensity during embryonic development (Fig. 4A). These changes in the fluorescence microscopic data were consistent with the changes in the fluorescent spectral data (Fig. 3). Based on these results, fluorescence emission was thought to originate from the mammillary knobs on the inner surface of the eggshell. Moreover, irradiation at 470–495 nm and 530–550 nm on the first day of embryonic development resulted in green and red fluorescent emission with reducing intensities by day 20 (Fig. 4B). The fluorescence properties of the inner surface of the eggshell, which emit blue, green, and red fluorescence when excited at specific and different

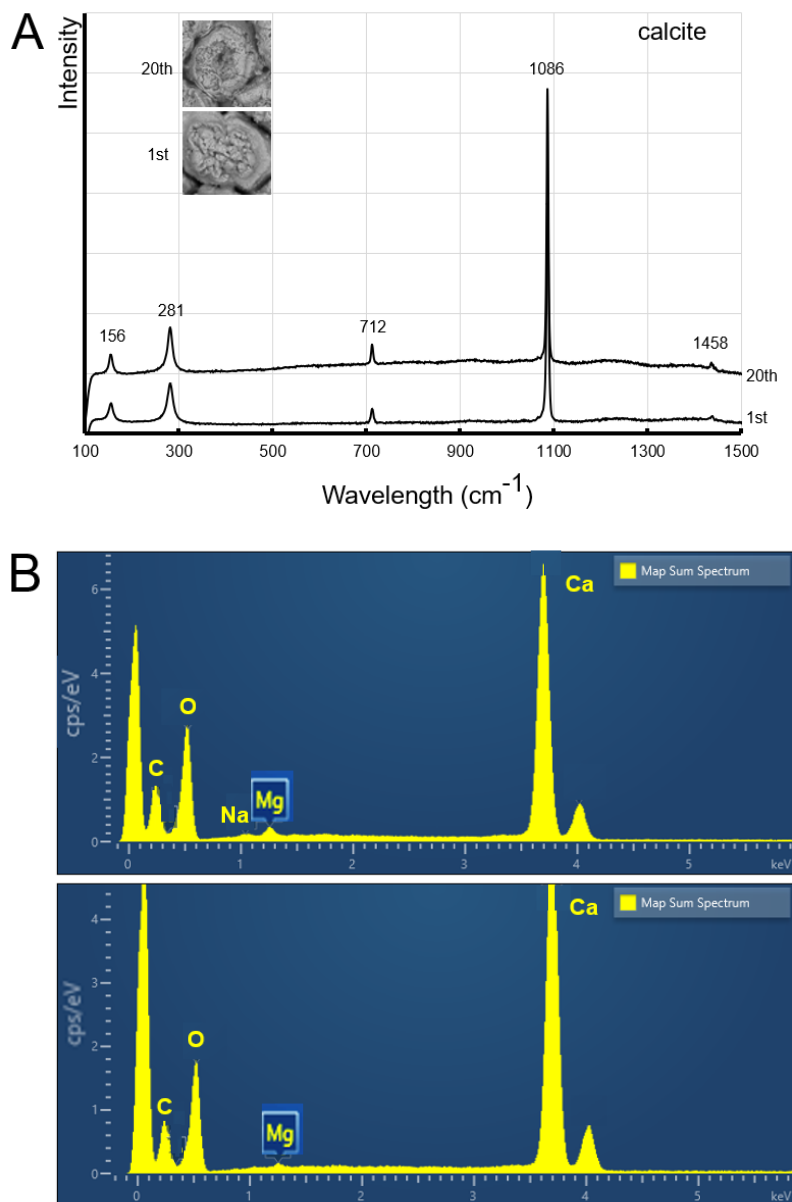


Fig. 5. Raman spectroscopic analysis and electron probe X-ray microanalysis (EDX) of the inside of a chicken eggshell.

A: Raman spectroscopic analysis; B: EDX. In these images, Raman spectroscopic and EDX data on the 1st and the 20th days during embryonic development were compared. Inserted photos in Fig. A indicate SEM images of the eggshell mammillary knobs on the 1st and the 20th days.

wavelengths, were remarkably similar to those of calcite crystals produced by the thermophilic bacterium *Geobacillus thermoglucosidasius*<sup>13</sup>. When comparing the Raman spectroscopy data on the inner surface of the eggshell (Fig. 5A) with the calcite data reported by Donnelly et al.<sup>14</sup>, the shift peaks almost matched. According to Donnelly et al.<sup>14</sup>, vaterite differs from calcite in that the peak at 1086 was a

double peak. Furthermore, according to Kupka et al.<sup>15</sup>, aragonite differs from calcite in that the peak near 712 was a double peak. By comparing the Raman shift peaks of calcite with aragonite and vaterite as described above, I confirmed that the mammillary knob was composed of calcite crystals rather than vaterite or aragonite. EDX elemental analysis during SEM observation revealed trace

amounts of magnesium and sodium ions in these calcite crystals, decreasing toward the end of embryonic development (Fig. 5B). Based on these fluorescence-related results as well as the Raman and EDX data (Figs. 4 and 5), I confirmed that the mammillary knobs were composed of fluorescent magnesium calcite crystals.

Recently, several studies have been conducted using abiotic reactions to assess how magnesium affects mineralization. Magnesium significantly influences  $\text{CaCO}_3$  precipitation, with sufficiently high magnesium concentrations producing aragonite precipitation and low Mg:Ca ratios incorporating magnesium into the crystal lattice to form calcite<sup>16,17</sup>. In addition, amorphous  $\text{CaCO}_3$  reportedly forms mesocrystals from calcite nanocubes while incorporating magnesium ions<sup>18</sup>. Mammillary knobs are also shaped like nanoparticle lumps, and small amounts of magnesium are thought to be incorporated into the crystal lattice during mammillary knob formation, resulting in lattice defects and misalignments that emit fluorescence<sup>19</sup>.

Various results have already been obtained concerning the changes in  $\text{CaCO}_3$  and  $\text{Ca}_3(\text{PO}_4)_2$  crystal properties upon incorporation of trace elements such as magnesium. For example,  $\text{CaCO}_3$  calcite crystals exhibit higher solubility when incorporating magnesium compared to pure calcite<sup>16</sup>. In addition,  $\text{Ca}_3(\text{PO}_4)_2$ -based hydroxyapatite becomes more soluble in acids with an increase in the amount of magnesium ions incorporated into the crystal<sup>20</sup>. Mammillary structures exist not only in chickens but also in various other birds, including ostriches<sup>21</sup>, quails<sup>22</sup>, and passerine birds<sup>23</sup>. In bird eggs, the easily soluble magnesium calcite on the inside of the eggshell could facilitate supplying the embryo with calcium, a building material for bones<sup>9,21</sup>, and magnesium, which controls cellular functions and enzymatic activities<sup>24</sup>, during embryonic development. Chicken eggshells contain various substances, such as  $\text{CaCO}_3$ , PPIX, and magnesium, as well as inositol phosphate<sup>21</sup> and various matrix proteins<sup>3</sup>. Future research efforts could unravel their new role and significance in embryonic development.

## Conclusion

The mammillary knobs of the inner surface of chicken eggshells are composed of fluorescent calcite crystals, which contain trace amounts of magnesium ions. These magnesium calcite crystals emit a blue fluorescence with a peak around 400–500 nm when exposed to 365 nm excitation light. When the same crystals are irradiated with 470–495 nm excitation light, they emit green fluorescence, and when exposed to 530–550 nm excitation light, they emit red fluorescence. These fluorescent characteristics bear a resemblance to those of calcite crystals formed by the thermophilic bacterium, *G. thermoglucosidasius*.

## Conflicts of Interest

The author has no competing interests to declare.

## Acknowledgments

I would like to thank Enago (www.enago.jp) for the English language editing.

## References

1. Kahil K, Weiner S, Addadi L, Gal A: Ion pathway in biomineralization: Perspectives on uptake, transport, and deposition of calcium, carbonate, and phosphate. *J Am Chem Soc*, 143: 21100-21112, 2021.
2. Tamamura Y, Yamaguchi A: Bone and tooth in calcium and phosphate metabolism [Jpn]. *Clin Calcium*, 22: 11-17, 2012.
3. Gautron J, Stapane L, Le Roy N, Nys Y, Rodriguez-Navarro AB, Hincke MT: Avian eggshell biomineralization: an update on its structure, mineralogy and protein tool kit. *BMC mol. Cell biol*, 22: 11, 2021. <https://doi.org/10.1186/s12860-021-00350-0>
4. Dauphin Y, Werner D, Corado R, Perez-Huerta A: Structure and composition of the eggshell of a Passerine bird, *Setophaga ruticilla* (Linnaeus, 1758). *Microsc Microanal*, 27: 635-644, 2021.
5. Okazaki T, Miyai S: Distribution of protoporphyrin and biliverdin in chicken and quail eggshells [Jpn]. *Int J Anal Bio-Sci*, 40: 168-175, 2017.

6. Sparks NHC: Eggshell pigments – from formation to deposition. *Avian Biol Res*, 4: 162-167, 2011.
7. Ishikawa S, Suzuki K, Fukuda E, Arihara K, Yamamoto Y, Mukai T, and Itoh M: Photodynamic antimicrobial activity of avian eggshell pigments. *FEBS Lett*, 584: 770-774, 2010.
8. Okazaki T, Miyai S: Changes in the fluorescence spectrum of protoporphyrin inside the eggshell and dissolution of the tip of the mammillary layer accompanied by chicken embryonic development [Jpn]. *Int J Anal Bio-Sci*, 45: 89-96, 2022.
9. Halgrain M, Bernardet N, Crepeau M, Mème N, Narcy A, Hincke M, Réhault-Godbert S: Eggshell decalcification and skeletal mineralization during chicken embryonic development: defining candidate genes in the chorioallantoic membrane. *Poultry Science*, 101: 101622, 2022.
10. Oral ÇM, Ercan B: Influence of pH on morphology, size and polymorph of room temperature synthesized calcium carbonate particles. *Powder Tec*, 339, 781-788, 2018.
11. Berg BL, Ronholm J, Applin DM, Mann P, Izawa M, Cloutis EA, Whyte LG: Spectral features of biogenic calcium carbonates and implications for astrobiology. *Int J Astrobiol*: 1-13, 2014. Doi: 10.1017/S1473550414000366
12. Toffolo MB, Ricci G, Caneve L, Kaplan-Ashiri I: Luminescence reveals variations in local structural order of calcium carbonate polymorphs formed by different mechanisms. *Scientific Rep*, 9:16170, 2019. Doi. Org/10.1038/s41598-019-52587-7
13. Yoshida N, Higashimura E, Saeki Y: Catalytic Biomineralization of fluorescent calcite by the thermophilic bacterium *Geobacillus thermoglucosidasius*. *Appl Environ Microbiol*, 76: 7322-7327, 2010.
14. Donnelly FC, Purcell-Milton F, Framont V, Cleary O, Dunne PW: Synthesis of CaCO<sub>3</sub> nano- and micro-particles by dry ice carbonation. *Chem Commun*, 53: 6657-6660, 2017.
15. Kupka T, Buczek A, Broda MA, Stobinski L: Modeling red coral (*Corallium rubrum*) and African snail (*Helix aspersa*) shell pigments: Raman spectroscopy versus DFT studies. *J Raman Spec*, 47: 908-916, 2016.
16. Loste E, Wilson RM, Seshadri R, Meldrum F: The role of magnesium in stabilising amorphous calcium carbonate and controlling calcite morphologies. *J Cryst Growth*, 254: 206-218, 2003.
17. Long X, Ma Y, Qi L: Biogenic and synthetic high magnesium calcite-A review. *J Struct Biol*, 185: 1-14, 2014.
18. Shang L-M, Jiang J, Yu S-H: Formation of magnesium calcite mesocrystals in the inorganic environment only by using Ca<sup>2+</sup> and Mg<sup>2+</sup> and its biological implications. *Sci China Mater*, 64: 999-1006, 2020.
19. Yasue T: Solid state chemistry on inorganic phosphor as host calcium salts [Jpn]. *Sikizai*, 74: 232-246, 2001.
20. Okazaki M, Takahashi J, Kimura H: Specific physico-chemical properties of apatites [Jpn]. Part 6. The effect of Mg<sup>2+</sup> ions. *JSDMD*, 5: 571-577, 1986.
21. Ito T, Kato S, Kubo A, Suematsu M, Nakata M, Saikawa Y: Small molecules assisting eggshell calcium dissolution for embryonic bone formation. *Tetrahedron*, 76: 130853, 2020.
22. Fathi MM, El-Dlebhshany AE, Bahie El-Deen M, Radwan M, Rayan GN: Effect of long-term selection for egg production on eggshell quality of Japanese quail (*Coturnix japonica*). *Poultry Sci*, 95: pew233, 2016.
23. Dauphin Y, Werner D, Corado R, Perez-Huerta A: Structure and composition of the eggshell of a passerine bird, *Setophaga ruticilla* (Linnaeus, 1758). *Microsc Microanal*, 27: 635-644, 2021.
24. Komiya Y, Su L-T, Chen H-C, Habas R, Runnels LW: Magnesium and embryonic development. *Magnes Res*, 27: 1-8, 2014.